

Fabrication and mechanical properties of glass fibre–carbon fibre polypropylene functionally gradient materials

JYONGSIK JANG*, CHOLHO LEE

Department of Chemical Technology, Seoul National University, San 56-1,
Kwanakgu Shinlimdong, Seoul, Korea
E-mail: jsjang@plaza.snu.ac.kr

Hybrid fibre mat reinforced polypropylene (PP) composites with carbon (CF) and glass fibre (GF) were prepared and four kinds of functionally gradient materials (FGM) were fabricated by changing the spatial distribution of GF and CF. To measure the mechanical properties of FGMs and hybrid composites, flexural tests and instrumented impact tests were performed. The flexural strengths and the flexural moduli of hybrid composites increased following the rule of mixture as the relative volume content of CF increased. On the other hand, the total impact absorption energy of hybrid composites decreased with the increment of CF relative volume content. Compared with GF–CF PP isotropic hybrid composite, the composites with compositional gradient showed similar flexural strengths, but characteristic flexural moduli. Especially, sandwich-type FGMs with a CF-rich outer layer and a GF-rich inner layer exhibited higher flexural moduli than others. Total impact absorption energies of four FGMs were also similar, but the ratios of crack initiation energy, E_i , to crack propagation energy, E_p , or ductility index, were quite different. © 1998 Kluwer Academic Publishers

1. Introduction

Glass fibre (GF) is widely used as composite reinforcement due to its low cost and excellent properties. It generally has a high strength-to-weight ratio, but its elastic modulus is low compared with fibres such as graphite and aramid [1]. Carbon fibre (CF) comprises one of the most important classes of reinforcement, with enormous potential for future growth. Its primary advantages over GF are higher modulus, lower density, improved creep rupture resistance and lower coefficient of thermal expansion. On the other hand, its fatigue energy is relatively low because of its low strain-to-failure ratio, and the impact resistance of CF composites is generally lower than that of GF reinforced composites. In addition, its general usage has been limited because of relatively high cost. In order to combine advantages of both GF and CF, these two fibres have been used as hybrid composites, which consist of two reinforcing fibres in a single matrix resin [2, 3].

Functionally gradient material (FGM) is a material that has a smooth transition from one material at one surface to another material at the opposite surface. Its concept was proposed by Niino *et al.* as a means of preparing thermal barrier materials usable not only in space structures and fusion reactors, but also in future space-plane systems [4]. FGMs generally consist of different material components and continuous changes in their microstructure distinguish FGMs from conventional composite materials. These structural changes

result in gradients in the properties of FGMs [4, 5]. Generally, the materials used widely are metals and ceramics that are combined in a controlled manner to optimize a specific property [6, 7]. This concept of ceramic–metal FGM can be applied to common fibre-reinforcement–polymeric-matrix composite, and the properties of composites with functional gradients will be different from those of composites without changes in their microstructure [8]. However, research in this field has not been performed extensively, and some functional gradients reported recently have been made only by the spatial distribution of reinforcing fibre and matrix resin.

In this paper, chopped CFs are added to GF reinforced thermoplastic composite (GMT) and four kinds of FGMs are fabricated by changing the spatial distribution of the two reinforcing fibres. The mechanical properties of hybrid composites that consist of FGM are measured. The effect of functional gradient on flexural and impact properties are investigated compared with GF–CF PP isotropic hybrid composites.

2. Experimental procedure

2.1. Materials

GF (ER1150 of Hankuk Fibre Glass Co., Korea) and CF (Torayca T300B from Toray Co., Japan) were used as the reinforcing fibres. The formation and properties of these fibres are shown in Table I. Both fibres were

* Author to whom correspondence should be addressed.

TABLE I Formations and properties of fibres

	Glass fibre	Carbon fibre
Diameter of monofilament, μm	22	7
Filament number in one yarn	3000	12 000
Elastic modulus, GPa	27.84	226
Tensile strength, GPa	0.94	2.94
Density, g m^{-3}	2.54	1.77

TABLE II Properties of PP matrix

	PP
Tensile strength, kgf cm^{-2}	380
Flexural modulus, kgf cm^{-2}	16 000
Flexural strength, kgf cm^{-2}	460
Izod impact strength at 23 °C, $\text{kg cm}^{-1}\text{cm}^{-1}$	7
Isotacticity, %	96.7
Density, g cm^{-3}	0.91

used without a desizing process or any surface treatment. The thermoplastic resin used in this study was PP (HF31E, Samsung Chemical Co., Korea). Its properties are shown in Table II.

2.2. Preparation of specimens

GF mats, CF mats and GF–CF isotropic hybrid mats were prepared using a custom-made fibre-mat-manufacturing machine, shown in Fig. 1. Fibre yarns were fed into the entrance with a feeding roller. As they went to the cutter, they were cut. Chopped fibres descended with the help of vacuum operation, and were spread and mixed to form a fibre mat at the perforated bottom screen of the machine. The relative volume content of CF–GF in GF–CF-mixed mats was varied by changing the feeding ratio of the two fibres. The average fibre length was set to 1 cm.

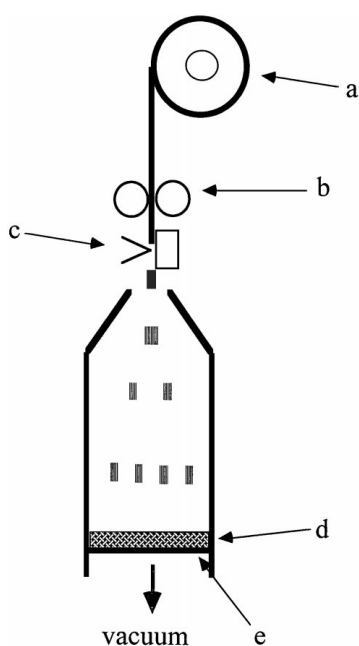


Figure 1 Schematic of the fibre-mat-manufacturing machine utilized in this experiment: (a) fibre roving, (b) feeding roller, (c) cutter, (d) fibre mat, (e) perforated screen.

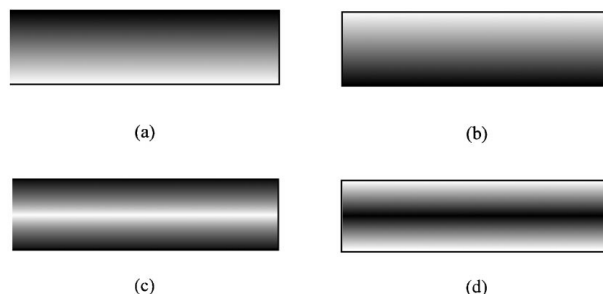
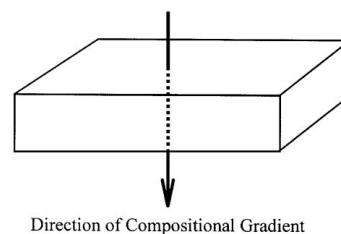


Figure 2 Schematic representation of functionally gradient materials fabricated in this experiment: (a) C : G, (b) G : C, (c) C : G : C, (d) G : C : G.

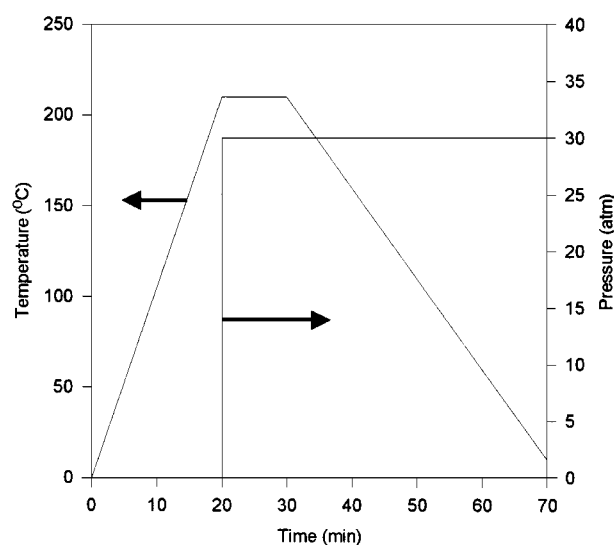


Figure 3 Temperature and pressure profiles for FGM manufacturing.

PP powder was dissolved in xylene at 140 °C and then the dissolved PP was poured into the fibre mats. After evaporating the solvent in a hood and vacuum oven for 24 h, 12 PP-impregnated prepreps were stacked to make GF–CF PP functionally gradient materials, as shown in Fig. 2. After stacking the prepreps, GF–CF PP FGMs were fabricated by compression moulding. Fig. 3 shows temperature and pressure profiles for manufacturing FGMs. In order to get the same degree of PP crystallization, cooling speed and pressure were kept constant during the cooling step [9].

Four types of GF–CF PP FGMs were fabricated and they were denominated as C : G, G : C, C : G : C, G : C : G, respectively. In the case of C : G, the relative volume content of CF–GF was 100% at the top layer and it decreased linearly to 0% at the bottom layer. In G : C, the direction of compositional change was reversed, or GF-rich layers were laid over CF-rich layers. C : G : C and G : C : G are sandwich-type FGMs. C : G : C has a

CF-rich shell and a GF-rich core, while G:C:G has a GF-rich shell and a CF-rich core. The total relative CF–GF content was equal to 50% in fibre mats and the net volume ratio of reinforcing fibres–matrix resin was 20% in all GF–CF PP FGMs.

2.3. Mechanical tests

To evaluate the mechanical properties of GF–CF PP FGMs, flexural tests and impact tests were performed. Specimens for three-point bending tests were prepared according to ASTM D790M. The dimensions of the flexural test specimens were $100 \times 10 \times 5$ mm, and the span length was set to 80 mm. Testing was performed with a crosshead speed of 2.1 mm min^{-1} . Seven specimens were tested using a universal testing machine (UTM, Lloyd LR10K). Flexural strengths and flexural moduli of hybrid composites were obtained from load–displacement curves. Impact testing was performed using an instrumented falling weight impact testing system (Radmana ITR2000). The dimensions of the impact specimens were $100 \times 100 \times 5$ mm. Five specimens or more were tested and the impact absorption energies obtained were divided by specimen thickness to normalize them. Crack initiation energies, E_i , and crack propagation energies, E_p , were calculated from each load–displacement curve.

2.4. Scanning electron microscopy (SEM)

A SEM was used to observe the fracture surfaces of GF–CF PP FGMs. The instrument used in this experiment was a Jeol JSM-35, and all specimens were coated with a thin layer of gold to eliminate charging effects.

2.5. Photographs

The deformation behaviour of FGMs was analysed using a manual camera after testing. Both the impacted surface and the back surface of FGMs were observed to examine the relation between the damaged shape and the absorbed impact energy.

3. Results and discussion

3.1. Mechanical properties of GF–CF PP hybrid composites

The flexural properties of GF–CF PP hybrid composites which consist of FGMs, are given in Fig. 4 as a function of CF volume fraction. As the relative volume content of CF in the GF–CF PP hybrid composite increases, the flexural strength and the flexural modulus increase. Although the CF PP composite yields catastrophically (see Fig. 5), it bears a higher load than the GFPP composite, resulting in a higher flexural strength. In addition, it deforms less until maximum load, which gives a higher flexural modulus. As a consequence, the flexural strength and the flexural modulus of the hybrid composite show larger values when the CF volume fraction increases. Furthermore, these flexural properties are proportional to CF content, or they obey the rule of mixture.

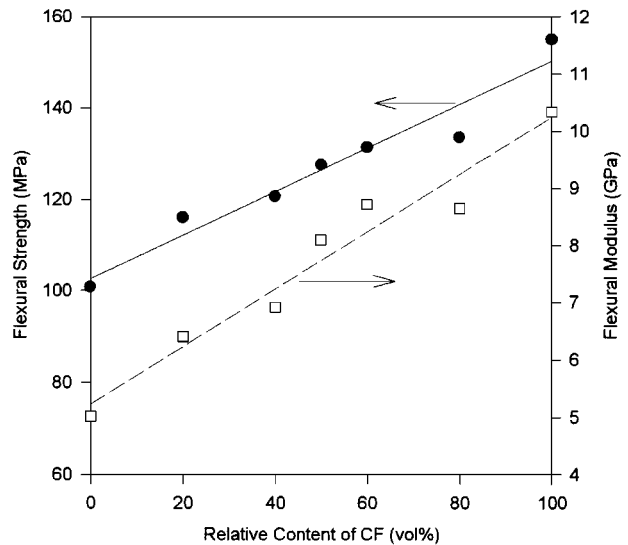


Figure 4 Flexural properties of GF–CF PP composites, which consist of FGMs, as a function of CF relative volume content: (●) flexural strength, (□) flexural modulus.

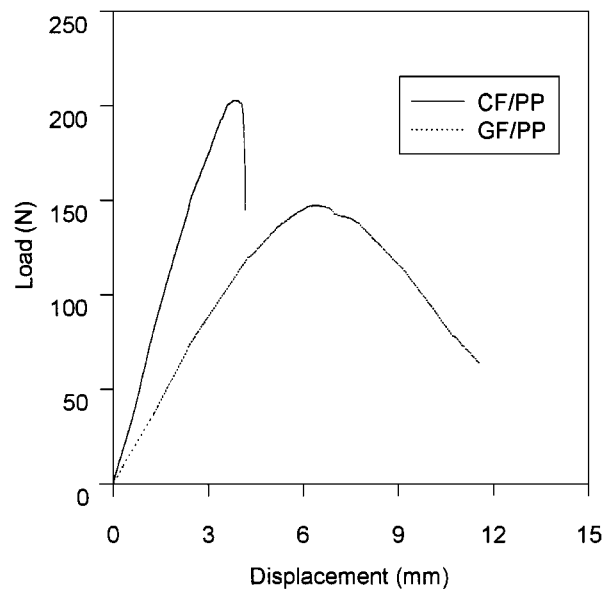


Figure 5 The load–displacement curves of CF PP composite and GF PP composite during flexural testing.

Fig. 6 represents the results of an instrumented impact test as a function of CF volume fraction in GF–CFPP hybrid composites. As CF content increases, crack initiation energies, E_i , decrease. Crack propagation energies, E_p , show the same trend. Due to these results, total absorbed impact energies, E_t , decrease with increasing CF content. Impact absorption energies are also proportional to the CF volume content, or they show linear decrement. This decrease is caused by the inferior impact toughness of CFs, which possess very low fracture strain values. The GF PP composite is compressed and deflected by the tip of the impactor in such a way that the specimen protrudes to form a dome along the rim of the penetrated hole as shown in Fig. 7a. During this process, many GFs are pulled out (Fig. 8a) and a matrix-whitening phenomenon, induced by fibre–matrix debonding, is observed near the hole surface (Fig. 7b). Deformation mechanisms, such

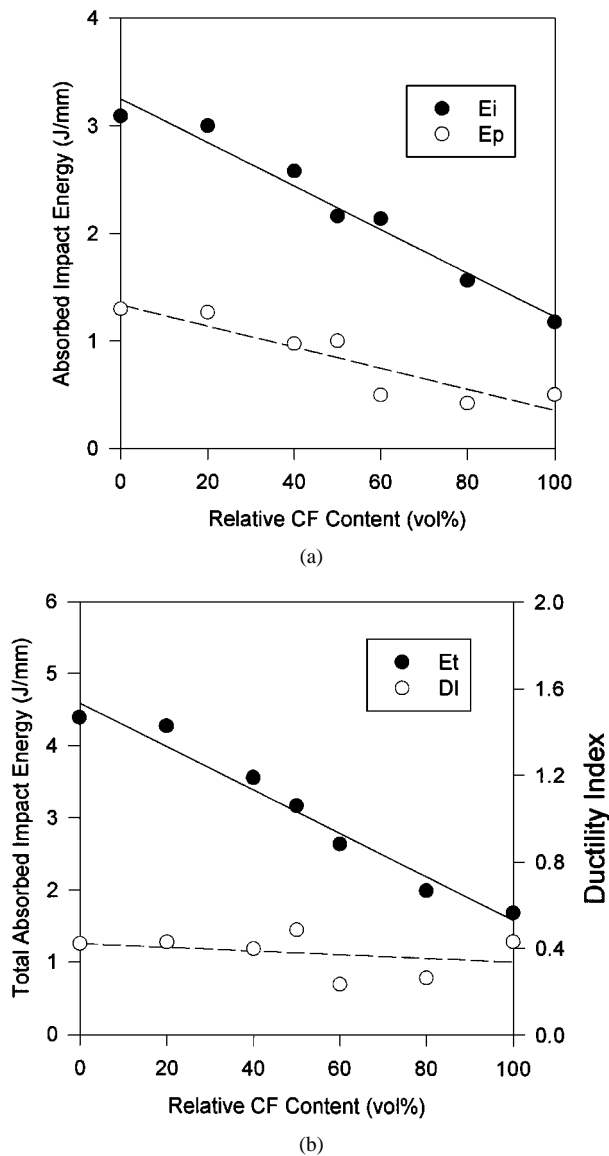
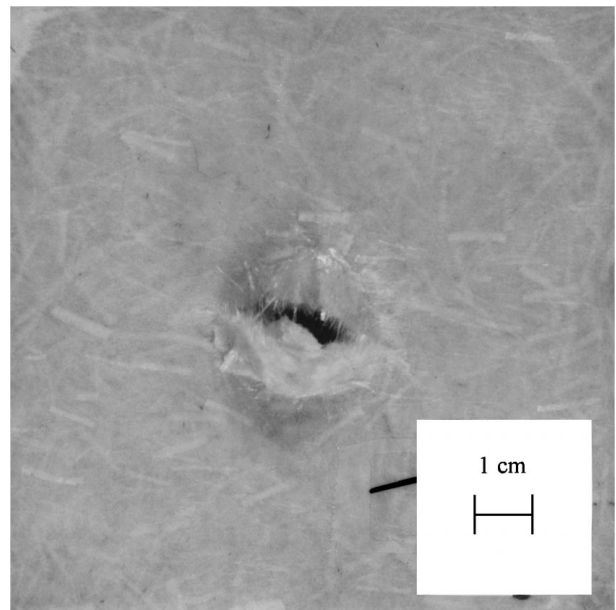
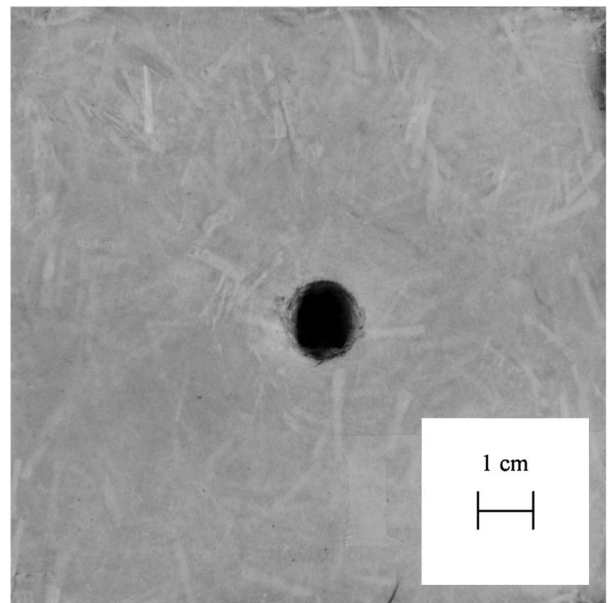


Figure 6 Impact properties of GF-CF PP composites, which consist of FGMs, as a function of CF relative volume content: (a) E_i and E_p , (b) E_t and DI.

as indentation, deflection and debonding, dissipate a significant amount of impact energy prior to perforation and penetration of the specimen by the impactor [10]. Therefore, the GF reinforced composite shows larger impact energy absorption. On the other hand, most of the CFs in the composite are broken rather than pulled out (Fig. 8a), and the pullout length of CFs is relatively short (Fig. 8b). The CF PP composite also forms a dome along the penetrated hole. This dome has a sharp boundary, while the GF PP composite has a smooth one (Fig. 9b). This also results from low strain-to-failure and a smaller degree of plastic deformation. From these facts, the CF PP composite has lower impact absorption ability. As a result, when the GF content decreases, the impact absorption energies of GF-CF PP hybrid composites show smaller values. The ratio of crack propagation energy to crack initiation energy, or the ductility index (DI) is similar, but decreases a bit with the increment of CF volume ratio, and we could say that the CF-rich GF-CF PP hybrid composite showed more brittle failure.



(a)

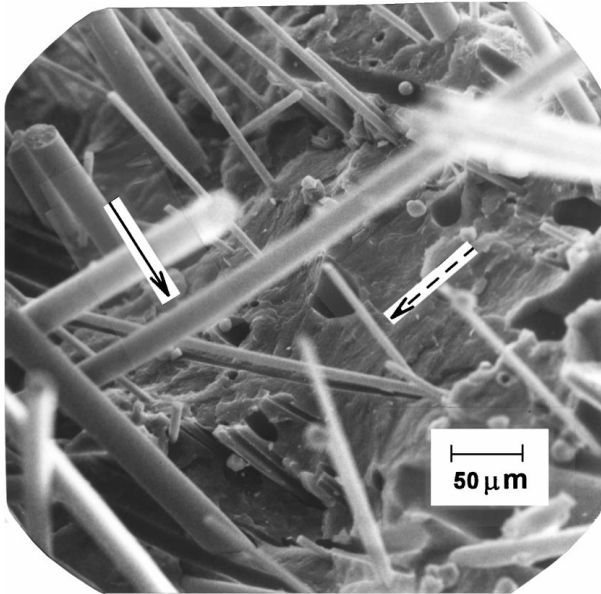


(b)

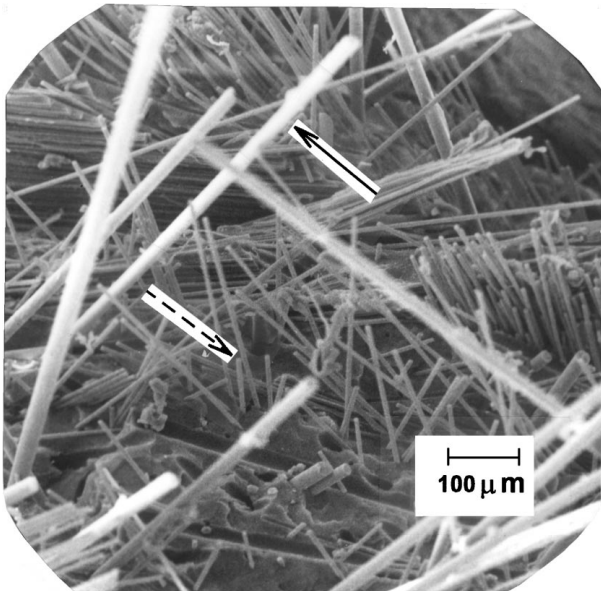
Figure 7 Photographs of GF PP composite after impact testing: (a) rear side, (b) front side—whitening phenomenon is observed.

3.2. Mechanical properties of functionally gradient materials

FGMs were fabricated by stacking GF-CF PP isotropic hybrid composites with different relative contents of CF. The flexural strengths changed insignificantly for the four kinds of FGMs, as shown in Fig. 10. But flexural moduli show characteristic values. C50 is the isotropic hybrid composite with equal amounts of GF and CF in volume ratio. This composite was fabricated to see the difference between an isotropic hybrid composite and FGMs. The highest flexural modulus is attained from the sandwich-type FGM with CF-rich shell and a GF-rich core (C : G : C). The lowest value results from G : C : G, which has a GF-rich outer layer and a CF-rich inner layer. During flexural testing, the shell sides are given high strain due to large compression and tension. If the relative volume fraction of high



(a)



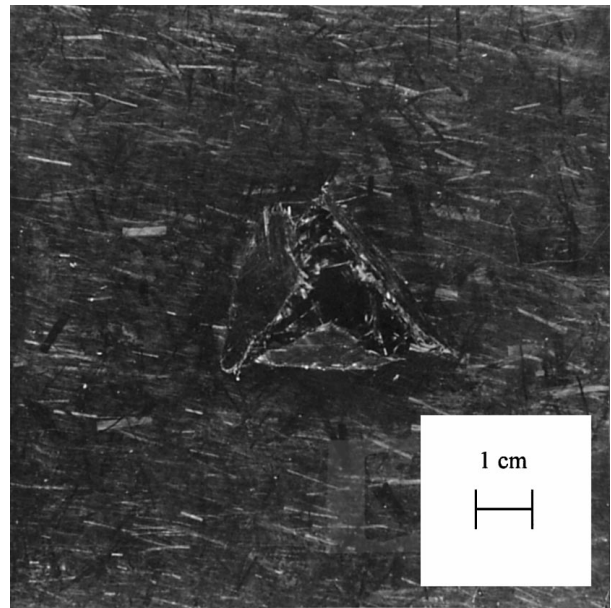
(b)

Figure 8 Scanning electron micrographs of the GF-CF PP hybrid composite after instrumented impact testing: (a) GFs are pulled out, (b) pull-out length of GF is longer than that of CF.

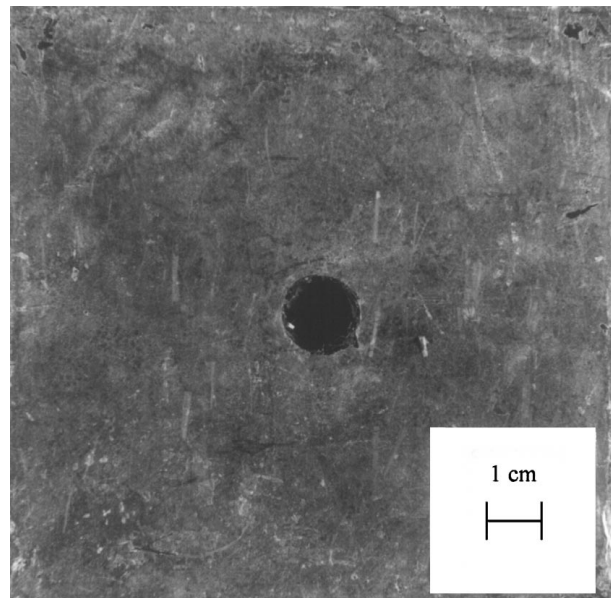
modulus CFs is high at the shell sides, the composite continues to resist the applied load up to a high value, resulting in high modulus. On the other hand, if the relative volume fraction of the low modulus GF is high at the skin portion, the composite deforms easily. As a result, lower flexural modulus is shown.

The results of the impact tests for GF-CF PP FGMs are given in Table III. Although the total impact absorption energies of these materials are similar, their failure patterns are quite different.

C : G exhibits low E_i and high E_p . The presence of the CF-rich layer restricts the ability of the GF-rich layer to deflect and deform plastically, and plastic deformation seems to occur by indentation of the front CF-rich layer. After maximum load, where perforation occurs in the CF-rich layer but not in the GF-rich layer, this composite is still capable of dispersing a considerable



(a)



(b)

Figure 9 Photographs of the CF PP composite after impact testing: (a) rear side – sharp dome is formed, (b) front side – whitening phenomenon is not observed.

TABLE III Impact absorption energies and ductility indices for GF-CFPP functionally gradient materials

FGM	Crack initiation energy, E_i (J mm ⁻¹)	Crack propagation energy, E_p (J mm ⁻¹)	Total impact absorption energy, E_t (J mm ⁻¹)	Ductility index (DI)
C : G	1.76	2.74	4.50	1.56
G : C	2.40	1.82	4.22	0.76
C : G : C	1.92	2.75	4.67	1.43
G : C : G	2.21	2.41	4.62	1.09
C50	2.11	1.74	3.85	0.82

amount of impact energy, leading to a relatively high E_p [11]. When the testing direction is changed, or the GF-rich side is set to front (G : C), high E_i and low E_p are obtained. The impact response of G : C appears to

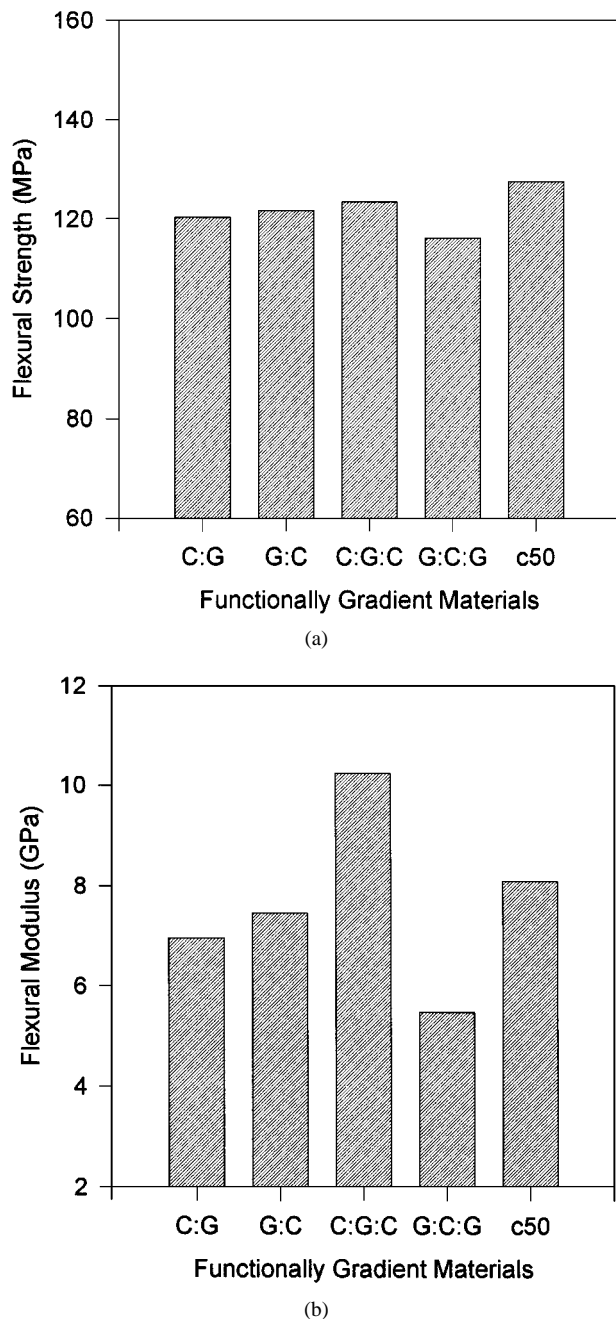


Figure 10 Flexural properties of GF-CF PP functionally gradient materials: (a) flexural strength, (b) flexural modulus.

be dominated by the front layer and a major portion of the impact energy is dissipated before the maximum load. In addition, the total impact absorption energy decreases compared with C : G. The CF-rich layer appears to have constrained the ability of the GF layer to undergo plastic deformation, thereby reducing its load-bearing and energy-absorbing capabilities [10].

In the case of a sandwich-type FGM with a CF-rich shell (C : G : C), low initiation energy and high propagation energy result. For C : G : C with a CF-rich skin and a GF-rich core, first fracture occurs on the compressive side. However, the strain in the tensile side is smaller and, therefore, additional deformation is required for the tensile face to reach tensile fracture [11]. By this reason, the propagation energy of the hybrid sandwich is large. For G : C : G with a GF-rich shell and a CF-rich core, high initiation energy and low propagation energy

are recorded. Compared with C : G, C : G : C had less CFs in the front layer, so GFs in the front layer could contribute to the initiation energy more. As a consequence, the C : G : C composite shows a higher initiation energy. In the G : C : G composite, the GF content in the front layer is lower than that of G : C, and by this fact E_i of G : C : G is lower.

4. Conclusions

GF-CF hybrid PP composites and four kinds of FGMs were fabricated by changing the spatial distribution of GF and CF. The mechanical properties of GF-CF PP hybrid composites, which consisted of FGMs, were measured. The flexural strengths and the flexural moduli of the hybrid composites increased following the rule of mixture as the CF relative volume ratio increased. On the other hand, the total impact absorption energy of the hybrid composites decreased with the increment of CF relative volume ratio.

Composites with compositional gradients showed similar flexural strengths to the GF-CF PP isotropic hybrid composite (C50), but characteristic flexural moduli. Especially, the sandwich-type FGM with a CF-rich outer layer and a GF-rich inner layer exhibited higher flexural modulus than others. The total impact absorption energies of the four FGMs were also similar, but the ratios of E_i to E_p , i.e. the ductility index, were quite different.

From these results, it is concluded that by fabricating FGMs and by choosing a proper compositional gradient, various or superior mechanical properties can be obtained, compared with isotropic hybrid composites.

Acknowledgements

This work was supplied by Korea Science and Engineering Foundation (No. 95-0300-02-04-3).

References

1. D. HULL, in "An Introduction to Composite Materials" (Cambridge University Press, NY, 1985).
2. C. ZWEBEN, H. T. HAHN and T. W. CHOU, in "Mechanical Behavior and Properties of Composite Materials" (Technomic Publishing).
3. N. L. HANCOX, in "Fibre Composite Hybrid Materials" (Applied Science, London).
4. J. B. HOLT, M. KOIZUMI, T. HIRAI and Z. A. MUNIR, in "Ceramic Transactions: Functionally Gradient Materials," Vol 34 (The American Ceramic Society, Westerville, OH).
5. K. M. JASIM, R. D. RAWLINGS and D. R. F. WEST, *J. Mater. Sci.* **28** (1993) 2820.
6. A. J. MARKWORTH, *ibid.* **30** (1995) 2183.
7. M. NIINO and S. MAEDA, *ISIJ Int.* **30** (1990).
8. M. FUNABASHI, in Proceedings of the Fourth Japan International SAMPE Symposium, September 1995.
9. J. KARGER-KOCSIS, in "Polypropylene: Structure, Blends and Composites" (Chapman & Hall, London).
10. B. Z. JANG, L. C. CHEN, C. Z. WANG, H. T. LIN and R. H. ZEE, *Compos. Sci. Technol.* **34** (1989) 305.
11. S. FISCHER and G. MAROM, *ibid.* **28** (1987) 291.

Received 21 July 1997

and accepted 30 July 1998